RSC Advances

PAPER

View Article Online
View Journal | View Issue

Cite this: RSC Adv., 2015, 5, 39482

pH dependent chemical stability and release of methotrexate from a novel nanoceramic carrier†

Sayantan Ray,[a] Mathew Joy,[a] Biswanath Sa,[b] Swapankumar Ghosh[a] and Jui Chakraborty*[a]

Considering the pH dependent chemical stability of anticancer drug methotrexate (MTX), the present communication reports a new approach for intercalation of the same in a nanoceramic vehicle, magnesium aluminium layered double hydroxide (LDH), by *ex situ* anion exchange method at pH 7.00, using 0.3 M ammonium acetate solution for dissolution of the drug. This simple method ensures maximum stability of the drug at the above said pH, with no degradation byproduct (*e.g.*, N^{10}-methyl folic acid formed due to alkaline hydrolysis) under the given experimental conditions, compared to the similar approach, using 0.1 M sodium hydroxide solution, reported in our earlier work. Importantly, the above method leads to an enhanced drug loading of 32.3 wt%, compared to our previous reports. The cumulative release profile of MTX from LDH–MTX formulation in phosphate buffer saline (PBS) at pH 7.4 exhibited burst release initially which was taken care of by imparting a unique coating of poly(D,L-lactide-*co*-glycolide, PLGA) on the LDH–MTX nanostructure that reduces the toxicity due to local accumulation. Hence, the superiority of the above for use in cancer chemotherapy, over the conventional drug–polymer system has been established w.r.t the drug release profile and a possible hypothesis of the same has been suggested. The half maximal inhibitory concentration (IC_{50}) of the MTX drug used in this study has been determined and the same has been used to estimate the time dependent (24, 48, 72 and 96 h) efficacy of the MTX loaded samples with/without polymer coating, on human colon tumour cells (HCT-116).

Received 27th February 2015
Accepted 22nd April 2015

DOI: 10.1039/c5ra03546e

www.rsc.org/advances

Introduction

The versatility of methotrexate in different treatment procedures is well known,[1–3] although it was originally developed and continued to be used in chemotherapy, either alone or in combination with other agents.[4] Despite a plethora of new drugs being used in the first line treatment of cancer chemotherapy, methotrexate still remains a popular choice of drug for the treatment of osteosarcoma, head and neck and breast cancer. Most clinicians prescribe high-dose MTX (HDMTX) ($\geq$500 mg m^{-2}), used for central nervous system (CNS) prophylaxis in patients with high-risk lymphoma and for the treatment of osteosarcoma. The main toxicities of HDMTX are elevated serum transaminase levels and renal insufficiency, which can delay drug clearance.[5,6] To overcome these secondary toxicities, this drug basically is administered *via* intravenous route in cycles within a single day, which is extremely painful and unacceptable for a patient. Hence, controlled release delivery of the drug for an extended period of time is desirable that aids in reduction of the dosage frequency and the systemic toxicity. Further, chemical instability of the active component of the drug leads to substantial lowering of the quantity of the therapeutic agent in the dosage.[7] pH is one of the most important factors affecting the stability of a drug that in turn is a major criterion in determining its suitability for a particular application, as above.[8] At alkaline pH range, N^{10}-methylfolic acid is the degradation byproduct of MTX, by alkaline hydrolysis reaction.[9,10] Hence, it is customary to develop "pH-Rate profiles" for drugs to determine the pH at which they are most susceptible to degradation and then formulate at a different pH along with the use of buffers to minimize degradation.[11] Considering this, in the present report, we have used a neutral medium, 0.3 M ammonium acetate of pH 7.00 for the first time, for dissolution of MTX, that aids to retain the pH dependent chemical stability of the pH sensitive drug so that no degradation by product, as above is formed and an enhanced drug entrapment efficiency is obtained.

In the rational design and evaluation of new dosage forms for drugs, a current approach encapsulates the chemically unstable, pH sensitive drug, methotrexate, in a delivery matrix that reduces the toxicity of the active pharmaceutical ingredient, when administered *via* intravenous route, and takes care of the pH sensitivity, as well. In this, a range of delivery matrices are

[a]CSIR-Central Glass and Ceramic Research Laboratory, 196, Raja S.C. Mullick Road, Jadavpur, Kolkata, 700 032, India. E-mail: jui@cgcri.res.in; Fax: +91-33-24730957; Tel: +91-33-24733476 ext. 3233

[b]Department of Pharmaceutical Technology, Jadavpur University, Jadavpur, Kolkata, 700 032, India

† Electronic supplementary information (ESI) available. See DOI: 10.1039/c5ra03546e

commercially available that are mostly polymers and have their intrinsic problems.[12] Among the matrices in use other than polymers, recently, a ceramic based nanoparticle known as layered double hydroxide (LDH) has received much attention in drug and gene delivery.[13–15] They are a class of natural and synthetic mixed metal hydroxides, anion exchanging clay-like materials, having chemical composition: $[M_{1-x}^{2+}M_x^{3+}(OH)_2]^+(A^{n-})_{x/n}\cdot mH_2O$, consists of brucite-like layers containing hydroxides of metal cations M^{2+} and M^{3+} and possess exchangeable anions, A^{n-} and a variable number of water molecules in interlayer space.[16] Due to anion exchange properties of LDH, many pharmaceutically active compounds, *e.g.*, NSAIDs, antineoplastic agents with an anionic counterpart, *e.g.*, ibuprofen, diclofenac, indomethacin, ampicillin, 5-flurouracil, methotrexate *etc.* have been intercalated into LDH brucite-like layers[17–23] and study on their sustained and controlled release, alongwith reducing systemic toxicity of the drug have been reported.[24–26] Despite the chemical instability of the MTX drug at alkaline pH (>8.0) conditions, a number of research groups have used 0.1 M sodium hydroxide solution for dissolution of the drug followed by its intercalation/insertion within the LDH layers.

In this regard, no reports could be obtained that examines the chemical stability of the intercalated drug and its effect in turn on the drug entrapment efficiency, under the said pH conditions. Further, LDH–MTX system leads to the release of the drug within a period of 24 h only which does not meet the requisite criteria of the chemotherapeutic agents that might effectively reduce the dosage frequency, toxicity and enhance patient compliance as well.

In view of the above, the present work reports the synthesis of LDH by simple co precipitation route and intercalation of the anionic counterpart of the anticancer drug methotrexate into the LDH interlayer by *ex situ* anion exchange technique, using 0.3 M ammonium acetate solution for MTX dissolution, at pH 7.00, at which the drug has maximum stability.[9,10,27] This exhibits enhanced drug loading (32.3 wt%) of the LDH–MTX system compared to our earlier results of 13.1 wt%. Hence, the superiority of ammonium acetate solution at pH 7.00, compared to sodium hydroxide solution at pH 8.5, for retention of pH dependent chemical stability of MTX during intercalation of the same by anion exchange process, has been demonstrated.[28,29]

The initial burst release and the local toxicity due to accumulation of the drug has been taken care by imparting a coating of poly(D,L-lactide-*co*-glycolide) (PLGA, 50 : 50) on the LDH–MTX nanohybrid by double emulsion ($W_1/O/W_2$)–solvent evaporation technique for the first time, to the best of our knowledge. The initial burst release (upto 2 h) of MTX drug that leads to dose dumping at the site, could be arrested by seven times approximately for the PLGA coated LDH–MTX compared to LDH–MTX alone. Analogous to PLGA–LDH–MTX, the PLGA–MTX counterpart, without LDH, was developed by single emulsion technique (O/W), using same amount of polymer. Significantly, the PLGA–MTX system exhibited complete release (99.9%) of MTX by a period of 5 days, compared to the LDH incorporated system (PLGA–LDH–MTX) that showed an extended release (99.5%) of MTX upto a period of 10 days, demonstrated by a schematic hypothesis. This extended release phenomenon of the PLGA–LDH–MTX for a period of 10 days helps to minimize the dosage frequency (*via* intravenous route in cycles within a single day) of HDMTX in cancer treatment, thereby, helps to get rid of the painful procedure of chemotherapy, alongwith its side effects and thus enhances patient compliance to a great extent. The nanoparticles (pristine/drug loaded/PLGA coated) and the PLGA–MTX system have been characterized using infrared spectrophotometry, scanning electron microscopy, dynamic laser scattering and thermogravimetric analysis-differential thermal analysis and scanning calorimetry. The drug loading, *in vitro* release and pH dependent degradation studies have been carried out in PBS medium at pH 7.4, using high performance liquid chromatograph (HPLC). Based on the half maximal inhibitory concentration (IC_{50}) of MTX drug, the time dependent (24, 48, 72 and 96 h) cell viability assay of the MTX loaded samples with/without polymer coating, on HCT-116 cells exhibited around six times higher efficacy for PLGA–LDH–MTX system compared to bare MTX drug, in a period of 96 h.

Experimental section

Materials

Methotrexate (molecular weight, 454.50 g mol^{-1}) was obtained as a gift sample from M/s Naprod Life Sciences, Mumbai, India. Magnesium nitrate hexahydrate, $Mg(NO_3)_2\cdot 6H_2O$, aluminum nitrate nonahydrate, $Al(NO_3)_3\cdot 9H_2O$, sodium hydroxide, NaOH and ammonium acetate, CH_3COONH_4 were purchased from M/s Sigma Aldrich, Bangalore, India. The polymer used in this work, poly(D,L-lactide-*co*-glycolide) (PLGA), with a copolymer ratio of D,L-lactide to glycolide of 50 : 50 (molecular weight in the range, 24 000–38 000 g mol^{-1}) (M/s Boehringer Ingelheim Pharma Gmbh & Co., Germany). The emulsifier poly(vinyl alcohol, PVA) and the solvent dichloromethane (DCM) were purchased from M/s Sigma Aldrich, St. Louis, MO, USA. Deionised and decarbonated ultrapure water (Millipore, specific resistivity 18.2 MΩ) was used in all the syntheses as above and the chemicals utilized in this study were used as received without further purification. The nitrogen gas used for synthesis and characterization in the present work is XL grade having percentage purity, 99.999%.

Preparation of the pristine LDH

32 mmol of $Mg(NO_3)_2\cdot 6H_2O$ and 16 mmol of $Al(NO_3)_3\cdot 9H_2O$ were dissolved in 500 ml decarbonated water maintained at 40 °C with stirring under a stream of nitrogen (XL grade, % purity, 99.999) gas. The pH of the resulting mixed metal solution was adjusted to 11.3 with 0.5 M of NaOH solution to get pristine LDH suspension that in turn was aged in the mother liquor for 24 h at room temperature under a nitrogen gas blanket, centrifuged (Heal Force, Neofuge 15R, China) at 9500 rpm for 5 min at 4 °C to separate the precipitate. The precipitate was washed several times with decarbonated water, freeze dried (EYEL4, FDU2200, Japan, at −82 °C and 20 Pa pressure) to get fine, free flowing nanocrystalline pristine LDH, denoted as sample A.

Preparation of the LDH–MTX nanohybrid by *ex situ* anion exchange technique

In ammonium acetate solution. A 100 ml solution of methotrexate (0.2% w/v) in 0.3 M ammonium acetate (pH 7.00) was added to 50 ml of aqueous suspension of sample A. The mixture was stirred (@1100 rpm) under nitrogen gas blanket for 48 h in a light protected condition at room temperature, followed by separation of the precipitate by centrifugation@9500 rpm for 8–10 min and washing several times with decarbonated water to remove the unbound drug. Next, the drug loaded nanohybrid formulation (LDH–MTX) was freeze dried and was named as sample B.

In sodium hydroxide solution. In this, a solution (100 ml) of methotrexate (0.2% w/v) in 0.1 M sodium hydroxide (pH 8.5) was added to 50 ml aqueous suspension of sample A, and the rest of the procedure is same as above, finally, the drug loaded nanohybrid formulation (LDH–MTX) was freeze dried and was named as sample B′.

To estimate the pH dependent chemical stability of MTX in sample B compared to sample B′, study of *in vitro* dissolution kinetics of the same was carried out at pH 7.4 using PBS medium.

Development of PLGA coating on LDH–MTX nanohybrid by double emulsion ($W_1/O/W_2$)–solvent evaporation technique

Coating of LDH–MTX by PLGA (50 : 50) was done using a double emulsion–solvent evaporation technique followed by high pressure homogenization.[30] An aqueous suspension (5 ml) containing 300 mg of LDH–MTX (equivalent to 100 mg of MTX present in sample B) was emulsified in 15 ml solution of PLGA (0.6 g PLGA in 15 ml dichloromethane), using a high speed homogenizer (IKA T25 ULTRA-TURRAX®, Germany) @12 000 to 15 000 rpm. The resulting water-in-oil (W_1/O) emulsion was transferred into a specific volume (50 ml) of an aqueous solution comprising 1% (w/v) poly(vinyl alcohol) used as an emulsifier.[31] The mixture was further emulsified for 2 min by homogenization (@8000 rpm) to obtain a double emulsion system. The solvent, dichloromethane was allowed to evaporate slowly at room temperature for a period of 12 h under agitation (@900 rpm) using a magnetic stirrer (IKA C-MAG HS7, Germany). The resulting PLGA coated LDH–MTX was collected by centrifugation at 8519*g* rcf (Heal Force, Neofuge 15R, China) for 10 min and was washed several times with decarbonated water followed by freeze drying (EYEL4, FDU2200, Japan, at −82 °C and 20 Pa pressure) to obtain a fine powder. This was named as sample C. Each of the above samples A, B and C were prepared in triplicate to check the reproducibility of the results. The amount of methotrexate present in sample B and C was quantified by HPLC analysis (see eqn (S1) and (S2) in ESI†).

Development of PLGA–MTX nanoparticles by single emulsion (O/W)–solvent evaporation method

Briefly, 200 mg of methotrexate and 400 mg of PLGA were dissolved in 5 ml acetone, and the resulting drug-polymeric solution was added slowly, drop by drop through a 16 gauge needle in 15 ml of aqueous phase containing surfactant solution, poly(vinyl alcohol, 1% w/v) under high speed homogenization at 13 500 rpm for 5 min.[32] The resulting O/W emulsion formed as above was stirred for a period of 8 h for complete evaporation of the solvent. The resulting suspension was centrifuged at 8519*g* rcf for 15 min and washed several times with decarbonated water. Finally, the particles were resuspended in a cryoprotectant (mannitol solution) and freeze dried at −80 °C for 12 h with a vacuum pressure of 20 Pa. This was named as sample D. The amount of methotrexate present in sample D was quantified by HPLC analysis (see eqn (S3) in ESI†).

In vitro dissolution study of sample B and B′

To estimate the time dependent degradation of the active drug present in sample B and B′, intercalated under two different pH conditions, 7.00 and 8.5, respectively, known quantities of the samples B and B′ (comprising methotrexate equivalent to 25 mg of active drug *via* intravenous route in single dose for treatment of cancer) were dispersed in 100 ml of phosphate buffer saline (pH 7.4) and at specific time intervals 5 ml of aliquots were withdrawn and replenished with the same. The aliquots were collected and was filtered through the membrane filter as above and were quantified using HPLC.

In vitro drug release study of MTX from samples B, C and D

In vitro drug release of MTX from samples B, C and D were carried out using type-II USP dissolution test apparatus (Electrolab TDT-146 08L Mumbai, India). In this, 0.086 g of sample B, 0.158 g of sample C (same as above) and 0.190 g of sample D were placed in a dialysis tubing cellulose membrane bag (cut off molecular weight 14 kD, M/s Sigma-Aldrich, St. Louis, MO 63178 USA) separately and immersed in 900 ml of PBS (pH 7.4) maintained at 37.2 °C with constant stirring@100 rpm.[33] At specific time intervals, 10 ml of aliquot was withdrawn and replenished immediately. The aliquots were filtered using a 10 ml luer lock syringe (part no. 008962, SGE Analytical Science, Victoria, Australia) with a 13 mm plastic Swinney filter holder (part no. NR 013100, Pall Corporation, USA) through a 0.2 mm, 13 mm dia Nylon 66 filter paper (Pall Corporation, USA). The filtered solution mentioned above was injected into the injection valve (injection volume: 10 μl) of the chromatograph (HPLC 820 Metrohm AG, Herisau, Switzerland). The retention time of the MTX drug in the column was recorded against the absorbance of the same using the UV-VIS detector (Lambda1010 Bischoff, Switzerland, wavelength range 190–800 nm). The mobile phase used for the analysis was a mixture of tris buffer : methanol : acetonitrile (80 : 10 : 10 v/v, pH 5.7), at flow rate of 0.8 ml min^{-1} at λ_{max} 313 nm. Before the analysis as above, the HPLC was calibrated using standard solutions of MTX in the concentration range 10–100 ppm. The calibration curve was generated with five known concentrations of the drug as above against its corresponding peak area derived from the chromatograms (Fig. 7A).

In vitro bioassay

Cell culture. Colon cancer (HCT-116) cells were obtained from ATCC (Rockville, MD, USA). All the cell lines were routinely cultured in DMEM (Invitrogen, Carlsbad, USA) supplemented with 10% heat-inactivated fetal bovine serum (Gibco, Invitrogen, UK), 2 mg ml^{-1} sodium bicarbonate, 1 μg ml^{-1} penicillin G and 1 mg ml^{-1} streptomycin, in 10 cm diameter plastic Petri dishes at 37 °C in a humidified atmosphere with 5% CO_2 in an incubator (HF90 Heal Force, China). The cells were subcultured using trypsin–EDTA when they were 90–95% confluent.[34] All experiments were done with the cells when they were within seven passages after revival from cryopreservation.

Determination of IC_{50} of MTX on HCT-116 cell line

The IC_{50} of MTX was evaluated at different concentrations in the range 5–40 μg ml^{-1} (ref. 35) with a stock solution of MTX (1 mg ml^{-1}) in dimethyl sulfoxide (DMSO, GR grade, Merck, India). To this, 1×10^4 HCT-116 cells per ml per well were plated in a 96-well plate. The cells were then incubated at 37 °C in the CO_2 incubator for 24 h to allow sufficient cell adhesion, and the incubation was continued for a total duration of 72 h after addition of MTX to the extent 5, 10, 15, 20, 25, 30, and 40 μg ml^{-1} (in triplicate). Cultured HCT-116 cells (1×10^4 cell per ml) in DMEM medium was taken as control. After 72 h, the MTT assay was performed by adding 10 μl of 3-(4,5-dimethylthiazole-2-yl)-2,5-phenyltetrazolium bromide (MTT) reagent at 1 mg ml^{-1} (Sigma-Aldrich, USA), in 1 : 9 ratio (MTT reagent : DMEM medium) to all the wells with subsequent incubation in dark for a period of 4 h at 37 °C. The reaction was stopped by adding 100 μl DMSO to each well of the plate after removal of the MTT and DMEM medium. The absorbance was then measured at 550 nm in an ELISA reader (Bio-Rad, USA), the dose response curves were generated and the HCT-116 cell sensitivity to MTX was expressed as IC_{50}.

Time dependent IC_{50} study of samples B, C and D

Briefly, 10 000 cell per well were taken in a 96 well plate, after 24 h incubation at 37 °C in humidified atmosphere containing 5% CO_2, the cells as above were treated with methotrexate loaded nanoparticles LDH–MTX, PLGA–MTX, PLGA–LDH–MTX, having MTX concentration (21 μg ml^{-1}), for 24, 48, 72 and 96 h (ref. 36) in the triplicate manner whereas cells which received 200 μl culture medium containing 5% DMSO served as control. We have carried out the study on half maximal inhibitory concentration (IC_{50}) of the active drug MTX loaded in three different samples, B, C and D upto an extended time point of 96 h, based on the controlled and slow release of MTX from polymer coated matrices (PLGA–LDH–MTX and PLGA–MTX) that indicates the possibility of better efficacy of the same in an extended time period.

Next, the cell viability was measured by MTT assay, as mentioned above and the absorbance of each well was read at 550 nm using ELISA reader (Bio-Rad, USA), to determine the efficacy of MTX in samples B, C and D respectively.

Instruments and characterization

Particle morphology and size of the samples A, B, C and D were examined by a Carl Zeiss SMT AG SUPRA 35VP (Germany) field emission scanning electron microscope (FESEM). The elemental composition of the samples (data not shown here) was studied using energy dispersive X-ray spectroscopy (EDX) attached to the FESEM. Particle size, polydispersity index (PDI) and zeta potential were measured using a Zetasizer Nano ZS (M/s Malvern, Worcs, UK) based on quasi-elastic light scattering. The samples were dispersed in deionized water and diluted 1/5 (v/v) with the same at room temperature. Zeta potential was measured using the same instrument at 25 °C following a 1/10 (v/v) dilution in deionised water. All the experiments as above were repeated at least three times to check the reproducibility of the results. Fourier-transform infrared spectra (FTIR) were recorded in a spectrophotometer (Perkin-Elmer Frontier™ IR/FIR, Waltham, USA) using KBr (M/s Sigma Aldrich, >99% pure) pellet (sample: KBr 1 : 100 by weight) spectrometer in the 400–4000 cm^{-1} range with average of 50 scans to improve the signal to noise ratio. Thermo gravimetric analyses (TG-DTA) of sample powders were carried out using a NETZSCH STA 409 CD thermal analyzer. The tests were carried out from ambient temperature to 1000 °C at a heating rate 10 °C min^{-1} in nitrogen atmosphere (flow rate 40 cm^3 min^{-1}). The physical compatibility of MTX drug entrapped in the sample B and C was determined by the differential scanning calorimetry (STA 449 F3 Jupiter®, NETZSCH, Germany). In this, ~5 mg of MTX, PLGA, sample B, sample C, physical mixture of MTX and sample A as placebo nanoparticles (MTX: sample A in 1 : 1 ratio by weight) were sealed in standard aluminum pans with lids and were heated from ambient to 500 °C (@5 °C min^{-1}) in nitrogen atmosphere.

Results and discussion

The pristine LDH was prepared by coprecipitation of the hydroxides of bivalent and trivalent metal ions at constant pH.[37] In this, the metal hydroxide with lowest solubility will precipitate out first, *e.g.*, $Al(OH)_3$ in the present case, while Mg^{2+} will remain in solution, subsequently leading to the precipitation of LDH as following:

$$2Mg^{2+} + Al^{3+} + 3OH^- \rightarrow Al(OH)_3(s) + 2Mg^{2+} \quad (1)$$

$$2Mg^{2+} + Al(OH)_3(s) + 3OH^- \rightarrow [Mg_2Al(OH)_6]^+ \quad (2)$$

In the above equations, water molecules are left out for simplicity. A schematic representation of the above reactions is shown below (Scheme 1).

The experimental yield of sample A was 16.7% sample B was ~49.74%, for sample C was ~67.03% and ~76.6% in case of sample D.

Fig. 1 depicts the FESEM images of sample A (LDH), sample B (LDH–MTX) and sample C *i.e.* PLGA coated LDH–MTX. Panel (a) shows cluster of flake/disk-shaped particles of size range 100–200 nm, distributed uniformly all over the sample in LDH. Both (a) and (b) panels exhibit the cross section view of some of

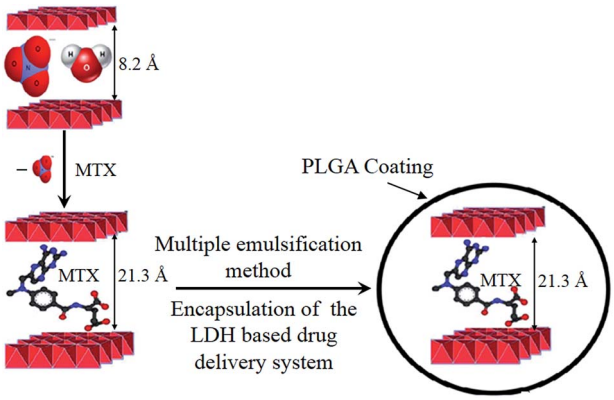

Scheme 1 Intercalation of MTX drug within the interlayer space of LDH, followed by coating of LDH–MTX using PLGA (50 : 50) exhibiting spherical shape of the drug loaded nanoparticle.

the particles (arrow marked) taking rod-like morphology for both LDH and LDH–MTX. On incorporation of the drug MTX, no major change could be noticed for the particle morphology and size distribution, as evident from panel (b).

Panel (c) shows uniform distribution of agglomeration free nanoparticles of PLGA polymer coated LDH–MTX, at low magnification (Fig. 1). Almost all the particles here have globular morphology, on being coated with PLGA. Nearly five times magnified image of a discrete PLGA coated particle as above in panel (d) clearly depicts the globular morphology and presence of the encapsulated LDH–MTX nanocluster (arrow marked) within the polymer coating. Additional images of the LDH–MTX aggregates followed by formation of agglomeration free PLGA coated LDH–MTX nanoparticles and PLGA coated MTX drug both at lower and higher magnification are given in Fig. S1 in ESI.†

The particle size affects the biopharmaceutical, physicochemical and drug release properties of the nanoparticles and

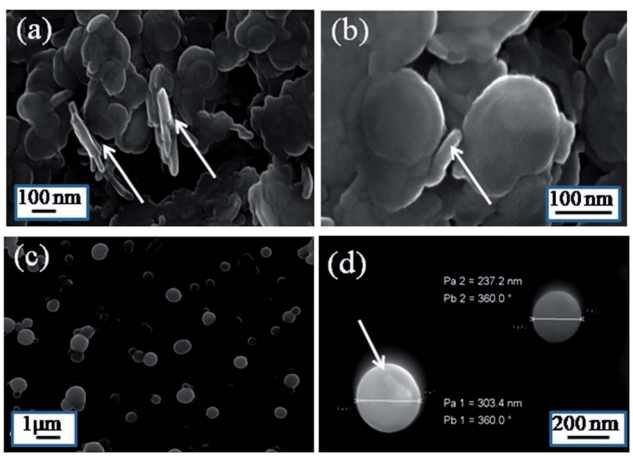

Fig. 1 FESEM micrographs of (a) pristine LDH (sample A), (b) LDH–MTX (sample B), (c) low magnification image of PLGA coated LDH–MTX (sample C) showing globular morphology of the nanoparticles, and (d) discrete globule shaped particles of PLGA coated LDH–MTX at higher magnification showing the presence of LDH–MTX nanoparticles within the polymer coating (arrow marked).

has direct relevance to the stability of the formulation. Smaller particles tend to aggregate fast,[38] thereby resulting in sedimentation. The pristine LDH particles were smaller than the MTX intercalated LDH nanoparticles which can be attributed to the increase in the gallery height on intercalation of the MTX drug in the interlayer space of LDH.

The pristine LDH and LDH–MTX nanoparticles exhibit unimodal distribution of the size in the range 50–120 nm. The D_{50} values of 60 nm and 80 nm of pristine LDH and LDH–MTX respectively with the polydispersity index (PDI) of 0.2 are indicative of a narrow distribution in the colloidal size range that could not be obtained earlier[39,40] and is attributed to an effective charge neutralization of the precipitated nanoparticles at neutral pH condition of the medium. Hence, as evident, majority of the drug loaded nanoparticles can reach the target cells[41,42] during drug delivery. Similar result on particle size distribution is presented in ESI (Fig. S2†). The variation in the colloidal stability, exhibited by the electrokinetic potential (ζ) in the range 43.20 to 19.01 mV for LDH and LDH–MTX respectively, as a function of surface charge, is indicative of intercalation of the anionic drug within the LDH interlayer, thereby, neutralization of the cationic charge of the brucite layers of LDH.[43]

Hence, the pristine LDH exhibits a good electrokinetic stability ($\zeta = 43.20$ mV) in the colloidal suspension comprising aggregation free nanoparticles in the cationic environment whereas the same for LDH–MTX indicate incipient stability ($\zeta = 19.01$ mV) on account of flocculation of the nanoparticles during the charge neutralization phenomenon as above. On encapsulation of MTX drug in PLGA nanoparticle, the average particle size was found to be in the range of 120–160 nm with D_{50} of 140 nm (Fig. 2A, panel c), and a PDI of 0.23 whereas, in case of LDH–MTX coated with PLGA, a unimodal size distribution was obtained in the range 150–300 nm with D_{50} of 200 nm, and a PDI of 0.35. The electrokinetic potential of −23.5 mV, in the later case indicates an incipient stability and is due to the presence of uncapped terminal carboxylic acid group of the PLGA polymer chains in the coated LDH–MTX nanoparticles.[44] The effect of emulsifier concentration in the process of emulsification is well known[45] that in turn influences both the particle size and zeta potential of the PLGA coated LDH–MTX nanoparticles, prepared by double emulsion–solvent evaporation technique in the present case. Importantly, the optimized concentration (Experimental section) of poly(vinyl alcohol), used as nonionic emulsifier here, plays a key role in masking the anionic chain extremities of the PLGA polymer,[46] (Scheme 2) thereby reducing the nanoparticle flocculation leading to a narrow particle size distribution and formation of a stable suspension as above. The difference in colours observed in layer b and c (Fig. 2B) is due non-matching refractive indices between LDH–MTX and PLGA polymer. See Table S1 of ESI† for detail information about a few related parameters.

The stretching vibrations at 1405 and 1609 cm^{-1} are attributed to C=C stretching of MTX, present in LDH–MTX in Fig. 3a. The broad hump at 3458 cm^{-1} in Fig. 3b is due to the stretching vibration of both structural hydroxyl and interlayer water molecules of the brucite layers.[43] The bands of medium

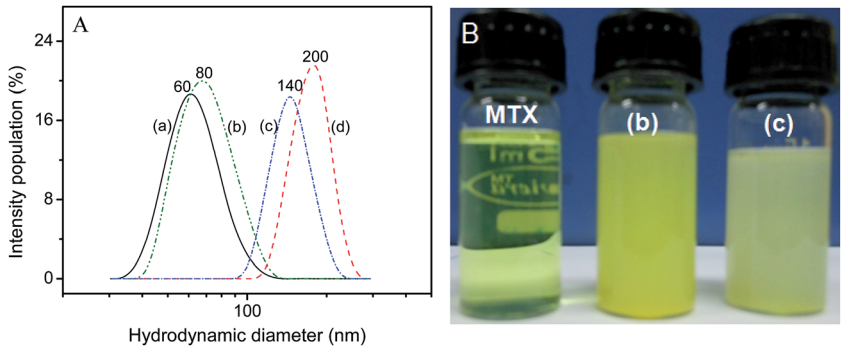

Fig. 2 (A) Particle size distribution (intensity) of (a) pristine LDH (sample A) (b) LDH–MTX (sample B) (c) PLGA–MTX (sample C) and (d) PLGA coated LDH–MTX (sample D) suspensions measured by dynamic light scattering technique. (B) Clear solution of MTX, showing transparent yellow colour, (b) stable suspension of LDH–MTX, showing lemon yellow colour and (c) PLGA coated LDH–MTX suspension, showing faint yellow colour. The solution/suspensions as above have been prepared at room temperature, using ultrapure water as medium.

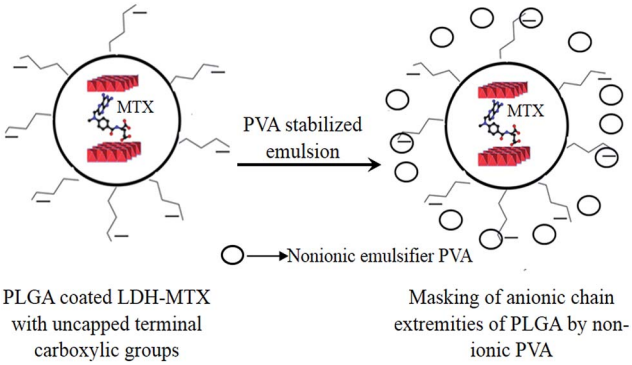

Scheme 2 The role of poly(vinyl alcohol) in masking the anionic terminal carboxylic groups of PLGA coating on LDH–MTX for a moderate zeta potential of the system.

intensity in the lower wave number region from 425 to 600 cm^{-1}, were due to M–O vibration and M–OH bending in the brucite-like layers,[40,43,47,48] while the presence of a strong band at 1392 cm^{-1} signifies the presence of NO_3^- anions in pristine LDH (Fig. 3b). The intensity of this band was reduced in LDH–MTX (Fig. 3a arrow marked), suggesting MTX intercalation leading to partial removal of NO_3^- anion. This is in corroboration with the presence of symmetric and asymmetric stretching vibration of COO^- (ν_{COO^-}) at 1380 and 1560 cm^{-1}, respectively, exhibiting MTX intercalation, as above. Other vibration bands of low and medium intensity are in line with our previous works.[39,40,43] The characteristics peak of MTX was showed (Fig. 3c) at 3460 cm^{-1} (–NH stretching), 1685 cm^{-1} (COOH), 1659 cm^{-1} (–CONH) and 850 cm^{-1} (aromatic stretch). Fig. 3d exhibits vibration bands of PLGA, due to stretching of alkyl group (2850–3000 cm^{-1}), carbonyl –C=O stretching (1700–1800 cm^{-1}), C–O stretching (1050–1250 cm^{-1}) and –OH stretching (3200–3500 cm^{-1}).[49] At 1755 cm^{-1}, the vibration band of medium intensity is attributed to –C=O stretching PLGA (Fig. 3, panel d) hydrocarbon chain, that remains unaltered in the spectrum corresponding to MTX and LDH–MTX loaded PLGA nanoparticles, as has been indicated by an elliptical shape in Fig. 3, panels d, e and f, indicating no chemical interaction/bonding between the PLGA coating and the encapsulated MTX/LDH–MTX. In addition to this, the vibration bands of low intensities corresponding to C=C stretching of MTX at around 1609 cm^{-1} is a good proof of the successful entrapment of MTX in PLGA in both the samples C and D (panels e and f of Fig. 3).

Fig. 4 shows the thermogravimetric curves (TG), carried out on LDH, MTX and LDH–MTX under air purge (thermooxidative analysis) condition. The hydrated pristine LDH powder shows a loss of 45.27% of its mass on heating upto 1000 °C. This loss corresponds to three decomposition steps at 125 °C, 250 °C and 410 °C, as is evident from the derivative plot of TG (Fig. 4A). The first decomposition step at 125 °C is attributed to the removal of surface adsorbed water molecules (13.75%), the second step corresponds to dehydroxylation of the structural water and the loosely bound exchangeable charge balancing anions that takes place in the temperature range 200–250 °C (8.6%). The remaining weight loss of 23.36% at 410 °C corresponds to the dehydroxylation during spinellization from hexagonal LDH moiety to an oxide lattice.[39,40,43]

The differential thermal analysis profile at panel (a) of Fig. 4B, exhibits an endotherm at 410 °C (ref. 43) corresponding

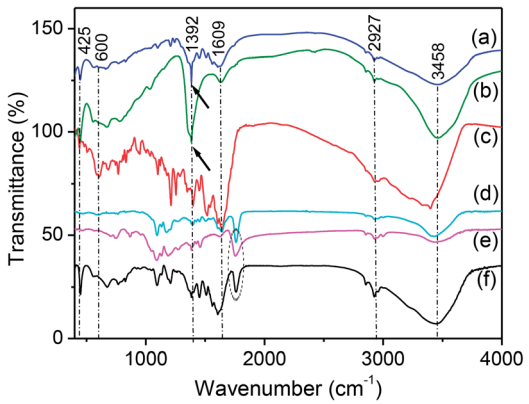

Fig. 3 FTIR spectra of (a) LDH–MTX (sample B), (b) sample A, (c) MTX, (d) PLGA (50 : 50) (e) PLGA coated LDH–MTX and (f) PLGA–MTX.

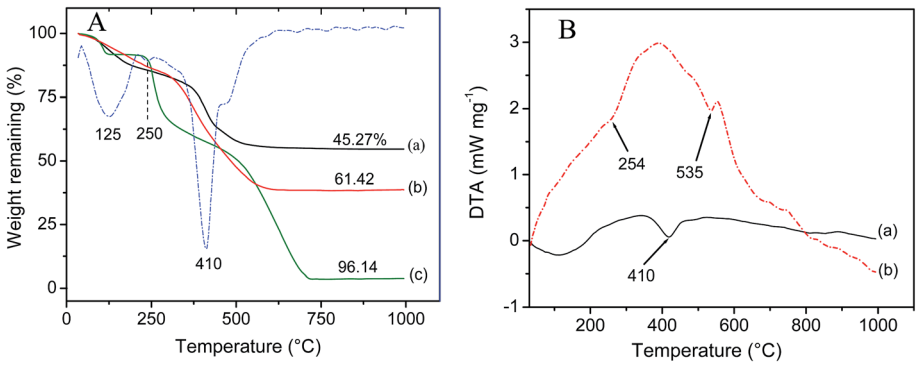

Fig. 4 (A) Thermogravimetry (TG) plots of (a) pristine LDH (sample A) and (b) LDH–MTX (sample B) (c) MTX. The derivative of TG data for LDH is shown as dotted line. (B) Differential thermal analyses of (a) pristine LDH (sample A) and (b) LDH–MTX (sample B).

to the decomposition of bound nitrate, carbonate ions and due to dehydroxylation during spinellization as above.[39,43] In case of LDH–MTX, the DTA pattern shows a small hump at 254 °C, that may be attributed to dehydroxylation of hydrogen bonded structural water. It indicates an enhanced thermal stability of the entrapped MTX drug, as evident from the melting point of bare MTX drug, in the range 195–210 °C.[50] The hump of medium intensity at 535 °C is attributed to the decreased strain energy of MgO nanocrystals on decarboxylation and decomposition of MTX drug in the interlayer space of LDH. The loading of MTX in LDH–MTX is estimated analyzing the thermogravimetric data,[51] as given below.

Let us assume 100 g of LDH–MTX contains 'x' g MTX of which $3.86x/100$ g will remain as residue after heating to 1000 °C and $(100 - x)$ g sample A of which $54.73(100 - x)/100$ g will be residue on heating to 1000 °C. So, $0.03863x + 4.73 - 0.5473x = 38.58$ (residue for LDH–MTX on heating to 1000 °C) which gives rise to 'x' as 32.3% MTX loading in LDH–MTX. The MTX loading data as above corroborates the same obtained from the HPLC analysis detailed in ESI,† to be 32 wt% approximately. Importantly, the MTX loading obtained by thermogravimetric analysis as above (data not shown here) for sample B′,[51] prepared in sodium hydroxide medium at alkaline pH (Experimental section) was 13.1% only. This may be attributed to the alkaline hydrolysis of MTX drug at pH 8.5 that leads to formation of degradation by product of N^{10}-methyl folic acid.[9,10] In case of sample C and D, the drug loadings are 56.60 wt% and 14.20 wt% respectively, obtained from HPLC analysis, detailed in ESI.†

Fig. 5 exhibits the differential scanning calorimetric (DSC) data of methotrexate, LDH–MTX physical mixture in 1 : 1 ratio by weight, LDH–MTX and LDH. Methotrexate thermogram in panel (a) shows a broad endothermic peak at around 200 °C, due to fusion of the hydrated form of the pure drug.[50] A minor shift in the peak as above to around 196 °C is observed in case of the LDH, MTX physical mixture (Fig. 5b), indicating intact physical state of the constituent compounds.

However, possibility of a weak interaction between MTX and its nanocarrier LDH, at higher temperature cannot be ignored here.[51,52] In case of LDH–MTX, the absence of the above peak, at panel (c) of Fig. 5, confirms the intercalation of methotrexate drug in the LDH interlayer. In case of bare PLGA, an endotherm at 220 °C confirms its fusion point in the temperature range 220–230 °C (ref. 53 and 54) whereas, on encapsulation of LDH–MTX/MTX the same could not be obtained on account of dilution of PLGA in the PLGA coated MTX/LDH–MTX as the composites contain less than 30% PLGA (TG(s) not shown here). A medium intensity endotherm at 373 °C corresponds decarboxylation during the spinellization process leading to nucleation of magnesium aluminate spinels and thereby

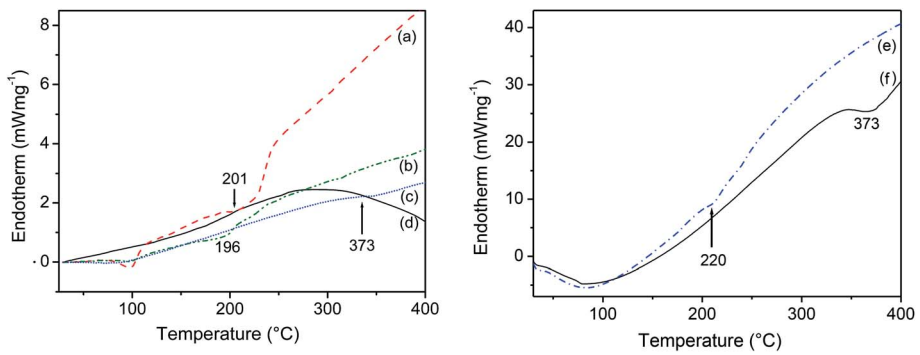

Fig. 5 Differential scanning calorimetry (DSC) of (a) MTX (API drug) (b) LDH : MTX physical mixture 1 : 1 ratio (c) LDH–MTX and (d) LDH. DSC of (e) PLGA and (f) PLGA coated LDH–MTX.

transformation of hexagonal LDH moiety to oxide spinels.[39,40,43] We obtained similar results from the TG-DSC data shown in panels (c) and (d) of Fig. 5 (arrow marked).

Fig. 6 demonstrates the time dependent (0.5 and 10 h here) HPLC analysis of samples B and B′, where MTX was intercalated in the LDH interlayer, under two different pH conditions of 7.00 and 8.5.[40,52] Initially, at 0.5 h, panel A exhibits the MTX concentration of 7.7 ppm, having retention time of 6.6 min, for sample B. In case of sample B′, at the same time point as above, a small peak showing retention time of 5.3 min and concentration 0.82 ppm, corresponds to N^{10}-methyl folic acid, the degradation by product of MTX (shown in Scheme 3), formed due to specific hydroxide ion-catalyzed reaction of the dianionic drug,[9,10,55] during intercalation into LDH layers under alkaline pH 8.5 condition, using 0.1 M sodium hydroxide solution. In case of sample B, in panels A and C, no such peaks are observed, on account of the maximum stability of MTX at pH 7.00, in ammonium acetate solution. Importantly, the concentration of the degradation byproduct of MTX drug, N^{10}-methyl folic acid, increases substantially with time: nearly six times (from 0.82 ppm at 0.5 h to 4.85 ppm at 10 h), as shown in panels D and E, in a period of nine and half hours (0.5 to 10 h) confirming the continued degradation process. The chromatograms of the intermediate time points (2, 4, 6 and 8 h) are demonstrated in ESI (Fig. S3†) that in turn, corroborates the above observation. Table S2 in ESI† has enlisted all the relevant parameters of the Fig. S3,† mentioned as above. The solid line through the scatter points is the linear fit to the data, exhibited in panel F.

The *in vitro* drug release from the above nanoparticles was studied by the dialysis membrane/bag diffusion technique. The dialysis bag retained nanoparticles and allowed the diffusion of drug immediately into the receiver compartment. The size of the nanoparticle also affect the drug release kinetics.[56] In Fig. 7B, layer (a) show complete (100%) release of MTX drug by a

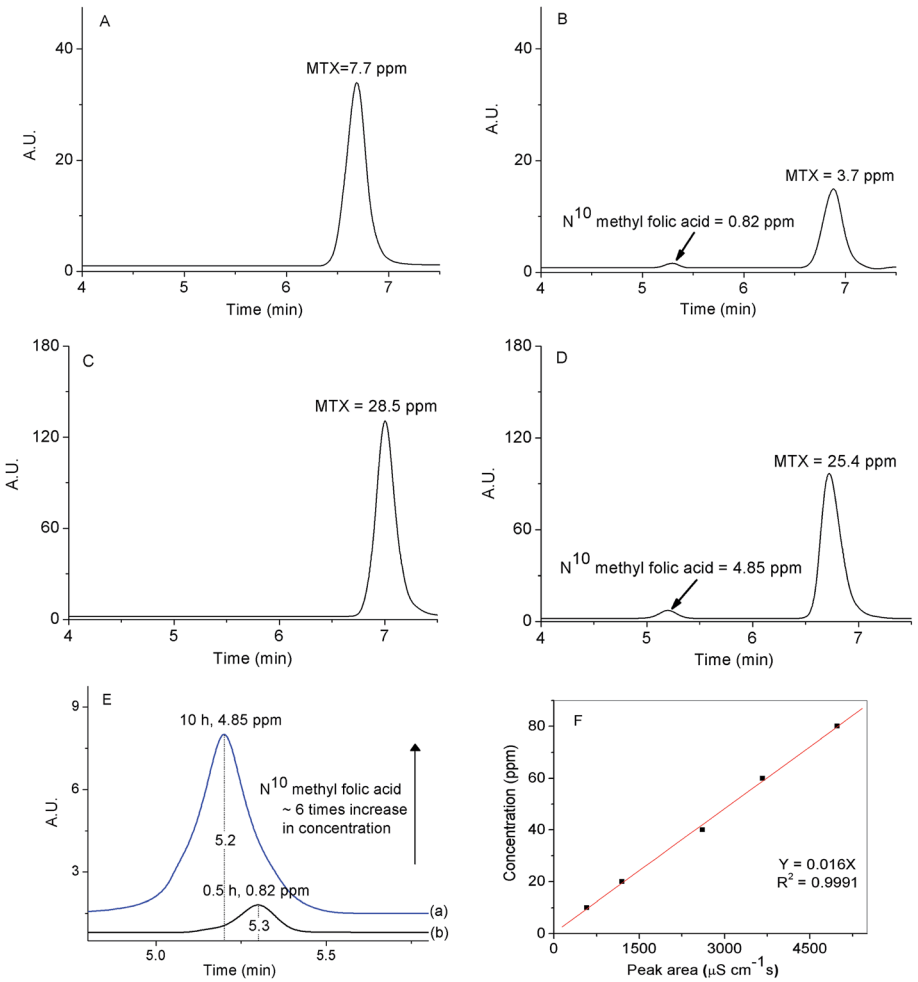

Fig. 6 Chromatograms showing the retention time in between 6.5–7.0 min for MTX release from LDH–MTX nanoformulation in PBS medium at pH 7.4: panel A showing the absence of any degradation peak (N^{10}-methyl folic acid) after 0.5 h of release of MTX from sample B. Panel B showing the presence of the peak as above for sample B′ (arrow marked). Panel C showing the absence of any degradation peak as above after 10 h of MTX release from sample B. Panel D showing the increased concentration of the degradation peak of sample B′ (arrow marked). Panel E showing the peak area of the degradation peaks of sample B′ at (a) 10 h and (b) 0.5 h of MTX release. Panel F showing the calibration curve of N^{10}-methyl folic acid concentration against the peak area. The straight line through the scatter plot is linear fit to the data. Table 1 demonstrates all the relevant parameters of the study as above.

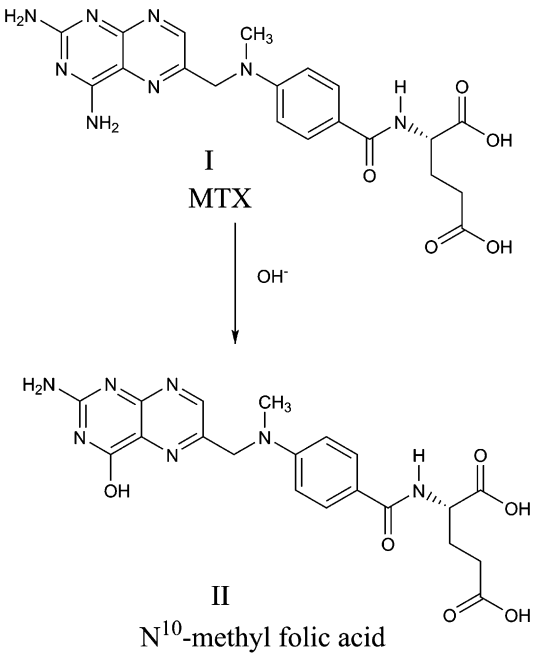

Scheme 3 Hydrolysis of MTX to form N^{10}-methyl folic acid in alkaline pH condition.

period of 2 h, due to absence of drug–carrier interaction in the physical mixture. In case of sample B (LDH–MTX), layer (b) shows the cumulative release in PBS at pH 7.4, which encompasses 99.7% of the drug by a period of 12 h. Of this, the release of 33–35% of the drug by a period of 2 h accounts for the loosely bound surface adsorbed drug, that leads to its local accumulation and hence, severe toxicity.[57] The remaining 65% of the release is attributed to the diffusion of MTX from the interlayer of LDH, by a fast anion exchange process in PBS medium, as shown in part A of Scheme 4. In case of sample D shown in layer (c) release of methotrexate from the PLGA nanoparticles consisted of two phases: phase 1 comprises the drug adsorbed on the surface of the polymer nanoparticles, leading to an almost linear release pattern whereas in phase 2, slow hydrolysis of the polymer in the release medium leads to loosening of the polymer chain and ultimately complete rupture of the same, as shown in step 2 and 2′ of Scheme 4, part B, resulting in slow and continuous drug diffusion through the pore, for a prolonged period of 120 h (5 days). In the present report, we have made an attempt to address the 'toxicity due to local accumulation' issue of the nephrotoxic drug MTX, as mentioned above, by imparting a thin polymer layer on the LDH–MTX nanoparticles, as detailed in the 'Experimental section'. Interestingly, a substantial reduction (~7 times) in the initial release rate (<5% by a period of 2 h, Fig. 7B, layer (d)) could be achieved along with extension of the release period approximately by two times compared to PLGA–MTX system and by twenty times compared to LDH–MTX system without any polymer coating. The possible mechanism for arrest of the release as obtained above is speculated in the following schematic hypothesis.

The polymer entrapped LDH–MTX (sample C),[58,59] initially, in contact with PBS at pH 7.4, hydrolysis of the PLGA matrix results in the polymer chain relaxation slowly, leading to release of the same in the dissolution medium. This immediately leads to anion exchange of the drug molecules with the phosphate

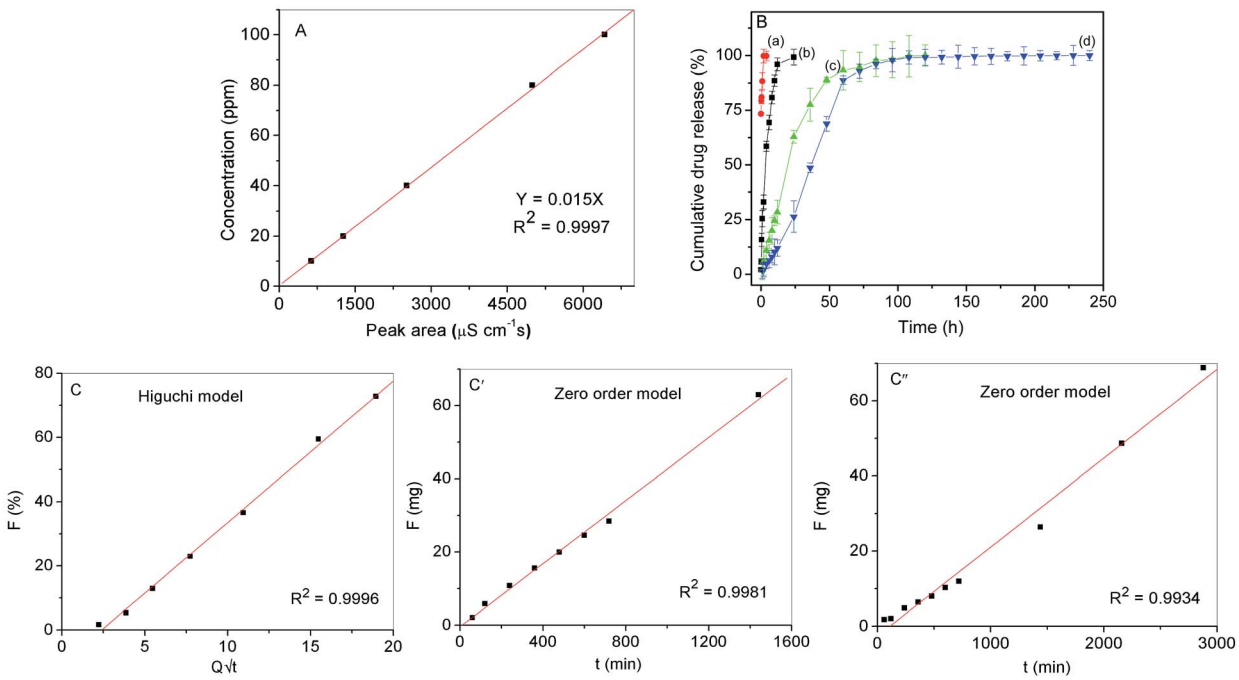

Fig. 7 (A) Calibration plot of methotrexate in phosphate buffer saline at pH 7.4. (B) Cumulative release profiles of MTX (a) physical mixture (LDH : MTX in 1 : 1 ratio by weight) and (b) LDH–MTX. (sample B) (c) PLGA–MTX. (sample D) and (d) PLGA–LDH–MTX (sample C). (C) Higuchi plot of sample B. (C′) Zero order plot of sample D. (C″) Zero order plot of sample C.

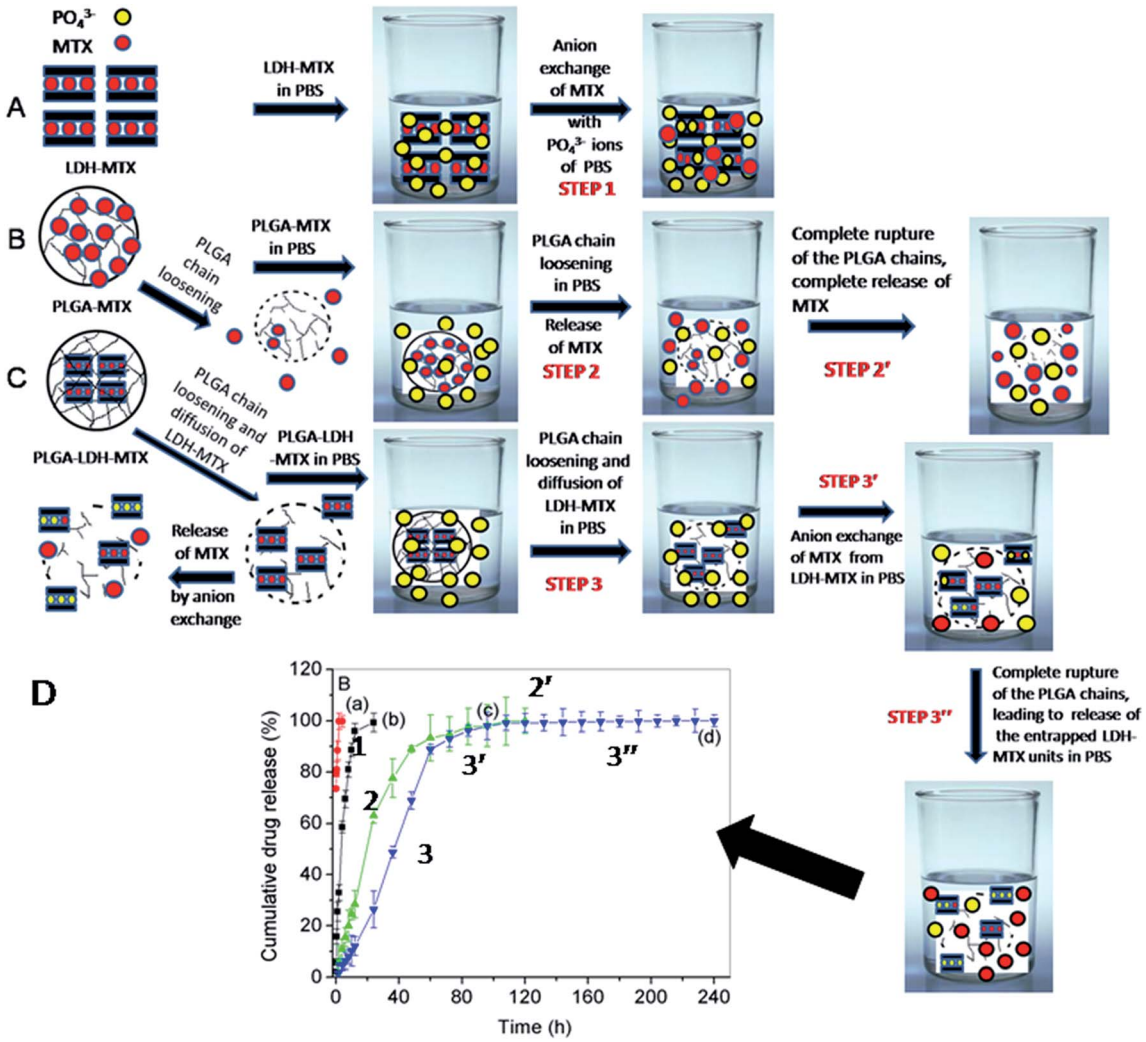

Scheme 4 Possible hypothesis of release of MTX from three different matrices of samples B, C and D.

ions of the PBS medium, as shown in step 3 and 3′of part C, Scheme 4 which is considered as phase 1 of the release, upto a period of 75–80 h, encompassing ~90% of the release, exhibiting superior performance of the system by its slow and controlled release profile, compared to PLGA–MTX in the time frame of 0 to 70 h. In phase 2 of the release, complete rupture of the polymer matrix, as shown in step 3″ of part C, Scheme 4, results in release of the remaining LDH–MTX units into the dissolution medium, followed by anion exchange phenomenon, as mentioned above. This part encompasses the remaining 9.5% of the release, upto a period of 160 h.

The analogy of various steps that have possibly taken place in the *in vitro* drug (MTX) release process of three different samples, B, C and D has been indicated in the obtained cumulative release profile, as shown in part D of Scheme 4, by the numericals, corresponding to the steps in Scheme 4.

The obtained *in vitro* release data as above were fitted in the release kinetic models: zero order, first order, Higuchi's square root plot, and Korsmeyer–Peppas[60–63] and the corresponding correlation coefficients and the kinetic exponents are presented in Table 2. Importantly, for sample B or LDH–MTX system, the Higuchi model of release is proposed based on the obtained R^2 value (0.9996), (Fig. 7C) indicating diffusion controlled release. In case of sample D and sample C, the same complies to zero order release model (R^2 = 0.9981 and 0.9934 respectively) which confirm the controlled release phenomenon that is independent of the drug concentration (Fig. 7C′ and C″).

Table 1 Variation in concentration and peak area, *versus* the retention time of the samples B and B′ as a result of *in vitro* dissolution study, at the time points, 0.5 and 10 h

	Concentration (ppm)		Peak area (mV s)		Retention time (min)	
	30 min	10 h	30 min	10 h	30 min	10 h
(a) Methotrexate						
Sample B	7.7	28.5	470.88	1962.3	6.6	6.85
Sample B′	3.7	25.4	230.77	1584.8	7.1	6.78
(b) N^{10}-methyl folic acid						
Sample B′	0.82	4.85	2.9	7.1	5.3	5.2

Table 2 Correlation coefficients (R^2) of different model of release kinetics of (LDH–MTX, PLGA–MTX and PLGA–LDH–MTX)

Formulation	Zero order	First order	Higuchi	Korsmeyer–Peppas	n values
LDH–MTX	0.9815	0.9991	0.9996	0.9914	0.382
PLGA–MTX	0.9981	0.9590	0.9657	0.9940	0.931
PLGA–LDH–MTX	0.9934	0.9917	0.9510	0.9910	0.948

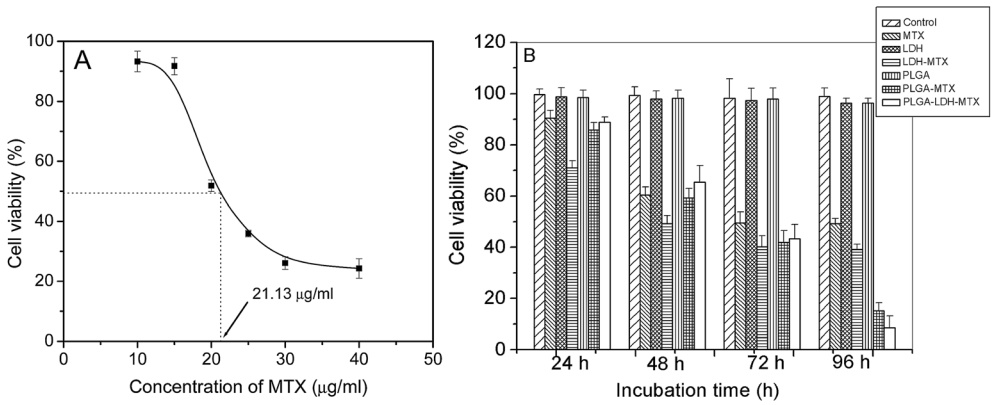

Fig. 8 (A) The half maximal inhibitory concentration (IC_{50}) of MTX using human colon tumour (HCT)-116 cell line. (B) Cell viability of samples B, C and D, alongwith MTX, LDH and PLGA nanoparticles.

Additional fitting plots of the drug release kinetics model are shown in Fig. S4 of ESI.†

The kinetic exponent 'n' for sample B (0.382) indicates the release following Fickian diffusion phenomenon, whereas the same for sample C and D systems are non-Fickian in nature. This is on account of an anomalous mechanism, in which the entrapped drug diffusion process is comparable to the relaxation rate of the polymer chain.[64–66]

Half maximal inhibitory concentration (IC_{50}) of MTX and *in vitro* cell viability assay of LDH–MTX, PLGA–MTX, PLGA–LDH–MTX

The IC_{50} of the MTX drug used in this study was determined to estimate the quantitative measure/concentration of the same to inhibit a given biological process by half. This can directly be correlated to the antagonist drug potency in the area of application. As per the result shown in Fig. 8 part A, the IC_{50} value of 21 μg ml^{-1} of MTX drug displayed a significant dose-dependent profile, after 72 h incubation. Considering the above concentration of methotrexate to attain the IC_{50} value, the cell viability assay of samples B, C and D were performed at four different time points, 24 h, 48 h, 72 h and 96 h and the result is shown in Fig. 8 part B. The time point 96 h was considered in our work, based on the controlled and slow release of MTX from polymer coated matrices (PLGA–LDH–MTX and PLGA–MTX) that indicates the possibility of better efficacy of the drug delivery system in an extended time period.

In a period of 48 h, the LDH–MTX nanoparticles inhibit the proliferation of 50% of the cells, compared to the same by a period of 72 h, in case of bare MTX drug. This can be attributed to the particle size alongwith the surface charge that leads to high affinity of the drug loaded nanoparticles and easy cellular uptake through the anionic cell membrane, by endocytosis mechanism. In case of polymer encapsulated MTX (PLGA–MTX), a similar effect (58% inhibition) as LDH–MTX is observed, compared to 56% in case of PLGA–LDH–MTX, in 72 h. This may be attributed to the slow release rate of methotrexate from the polymer matrices by chain relaxation and diffusion mechanism in both the cases. Interestingly, in a period of 96 h, the release of MTX at a continuous and controlled rate led to an excellent inhibitory efficiency both for PLGA–MTX and PLGA–LDH–MTX, compared to LDH–MTX and the bare drug, on account of intracellular drug accumulation as above, over a prolonged period of time. Finally, the biocompatible and biodegradable nanoceramic carrier, LDH and the polymer matrix PLGA are non toxic and can be completely metabolized,[67,68] hence, has no effect on the cell viability, as shown in Fig. 8 part B.

Conclusion

The present work demonstrates the pH dependent chemical stability of antineoplastic drug, methotrexate under two different pH conditions of 7.00 and 8.5, at which the dissolution of the drug was carried out using 0.3 M ammonium acetate and 0.1 M sodium hydroxide solutions respectively, for intercalation within the interlayer space of LDH. Interestingly, the *in vitro* dissolution study of the samples at the time points 0.5, 2, 4, 6, 8 and 10 h as above revealed the peaks corresponding to N^{10}-methyl folic acid, formed by alkaline hydrolysis of methotrexate, in the later case which was not obtained in the former case on account of the maximum stability of the

drug at neutral pH condition (pH 7.00). Further, in case of LDH–MTX, the drug loading at pH 7.00 is >two times (~32.3 wt% here) and for PLGA–LDH–MTX, it is >four times compared to the case undertaken at alkaline pH condition (13.1 wt%). The LDH–MTX nanoparticles have been coated with PLGA to arrest the initial burst release (33–35% by a period of 2 h), that leads to dose dumping at the site and thereby to reduce the toxicity due to its local accumulation. To establish novelty of the present approach, we developed PLGA coating on MTX drug by single emulsion–solvent evaporation technique, as well. Significantly, we obtained a two times extension of release of the drug in a controlled manner in case of PLGA–LDH–MTX (99.5% release in 10 days), compared to PLGA–MTX system (99.9% release in 5 days) explained on the basis of a schematic hypothesis. This extended release phenomenon of the PLGA–LDH–MTX for a period of 10 days helps to minimize the dosage frequency (*via* intravenous route in cycles within a single day) of HDMTX in cancer treatment, thereby, helps to get rid of the painful procedure of chemotherapy, alongwith its side effects and thus enhances patient compliance to a great extent. In general, a particle size distribution in the range 50–120 nm was obtained for LDH–MTX whereas, on coating with PLGA, the same was in the range 150–300 nm, indicating the possibility of reaching the target cells, in both the cases. FTIR analysis indicates partial reduction of the vibration frequency corresponding to the nitrate anion, on insertion of the drug macromolecule in the octahedral framework of LDH, followed by almost no shift in the characteristic vibration frequencies of PLGA, exhibiting absolute compatibility and no chemical interaction of the same with the coated MTX/LDH–MTX. This data corroborates with our DSC result which exhibits formation of an integrated drug delivery system, on coating of LDH–MTX nanohybrid particles with PLGA. The half maximal inhibitory concentration (IC_{50}) of the MTX drug, obtained as gift sample was 21.13 $\mu g\ ml^{-1}$ on human colon tumour cells and the same for the LDH–MTX systems with/without PLGA coating, showed the efficacy in the order, LDH–MTX > PLGA–MTX > PLGA–LDH–MTX in a period of 48 h, whereas, importantly, in a longer time gap of 48 h more, the order as above changes as, PLGA–LDH–MTX > PLGA–MTX > LDH–MTX (96 h). In summary, the present report elaborates the importance of neutral pH (7.00) condition for obtaining chemically stable antineoplastic drug MTX within the interlayer space of nanoceramic carrier, LDH, with better loading, as mentioned above, compared to our earlier reports. Further, the suitability of a biocompatible and biodegradable polymer (PLGA here) coating on the nanoceramic based (LDH–MTX) drug delivery system to arrest the initial burst release and extend the same in a controlled manner has been illustrated by a schematic hypothesis. The superiority of the PLGA–LDH–MTX system has been established compared to its polymer coated counterpart, *i.e.*, PLGA–MTX system, w.r.t the drug loading (% by wt) and release profile, and the work is primarily oriented to minimize the dosage frequency of extremely toxic MTX drug in cancer treatment and thereby improve patient compliance to a great extent.

Acknowledgements

The authors are grateful to the Director, Central Glass and Ceramic Research Institute, Kolkata, India for providing his permission and facilities to carry on the above work. Thanks are due to all the supporting staffs for various characterization works. Thanks are also due to Ms Rituparna Acharya, M.Phil fellow of Jadavpur University, for helping us in carrying out a part of the *in vitro* cell viability assay. This work was supported by the CSIR Twelve Five Year Plan Project ESC 0103 (BIOCERAM).

Notes and references

1 K. Foulmann, J. P. Guastalla, N. Caminet, V. Trillet-Lenoir, D. Raudrant, F. Golfier and A. M. Schott, *Gynecol. Oncol.*, 2006, **102**, 103.
2 N. M. Annest, M. J. VanBeek, C. J. Arpey and D. C. Whitaker, *J. Am. Acad. Dermatol.*, 2007, **56**, 989.
3 B. C. Widemann and P. C. Adamson, *Oncologist*, 2006, **11**, 694.
4 S. Ferrari, S. Smeland, M. Mercuri, F. Bertoni and A. Longhi, *J. Clin. Oncol.*, 2005, **23**, 8845.
5 M. A. Perazella and G. W. Moeckel, *Semin. Nephrol.*, 2010, **30**, 570.
6 R. G. Stoller, K. R. Hande, S. A. Jacobs, S. A. Rosenberg and B. A. Chabner, *N. Engl. J. Med.*, 1977, **297**, 630.
7 Y. Zhang, Q. A. Xu, L. A. Trissel and D. L. Gilbert, *Hosp. Pharm.*, 1996, **31**, 965.
8 Y. W. Chueng, B. R. Vishnuvajjala and K. P. Flora, *Am. J. Hosp. Pharm.*, 1984, **41**, 1802.
9 J. Hansen, B. Kreilgård, O. Nielsen and J. Veje, *Int. J. Pharm.*, 1983, **2**, 141.
10 D. C. Chatterji and J. F. Gallelli, *J. Pharm. Sci.*, 1978, **67**, 526.
11 V. Loyd and J. Allen, *Pharm. Globale*, 2011, **1**(8), 11.
12 V. Labhasetwar, C. Song and R. J. Levy, *Adv. Drug Delivery Rev.*, 1997, **24**, 63.
13 J. H. Choy, S. J. Choi, J. M. Oh and T. Park, *Appl. Clay Sci.*, 2007, **36**, 122.
14 K. Ladewig, M. Niebert, Z. P. Xu, P. P. Gray and G. Q. M. Lu, *Biomaterials*, 2010, **31**, 1821.
15 S. Aisawa, S. Sasaki, S. Takahashi, H. Hirahara, H. Nakayama and E. Narita, *J. Phys. Chem. Solids*, 2006, **67**, 920.
16 F. Li and X. Duan, *Struct. Bonding*, 2006, **119**, 33.
17 M. Trikeriotis and D. F. Ghanotakis, *Int. J. Pharm.*, 2007, **332**, 178.
18 V. Ambrogi, G. Fardella, G. Grandolini, M. Nocchetti and L. Perioli, *J. Pharm. Sci.*, 2003, **92**, 1407.
19 G. Fardella, L. Perioli, V. Ambrogi and G. Grandolini, *Proc. Int. Symp. Controlled Release Bioact. Mater.*, 1998, **25**, 774.
20 V. Ambrogi, G. Fardella, G. Grandolini and L. Perioli, *Int. J. Pharm.*, 2001, **220**, 23.
21 V. Ambrogi, G. Fardella, G. Grandolini, L. Perioli and M. C. Tiralti, *AAPS PharmSciTech*, 2002, **3**, 26.
22 S. J. Choi, J. M. Oh and J. H. Choy, *J. Nanosci. Nanotechnol.*, 2010, **10**, 2913.
23 T. H. Kim, G. J. Lee, J. H. Kang, H. J. Kim, T. Kim and J. M. Oh, *BioMed Res. Int.*, 2014, **1**, 1.

24 M. M. Ajat, K. Yusoff and M. Z. Hussein, *Curr. Nanosci.*, 2008, **4**, 391.
25 S. J. Choi, J. M. Oh, T. Park and J. H. Choy, *J. Nanosci. Nanotechnol.*, 2007, **7**, 4017.
26 S. J. Choi, J. M. Oh and J. H. Choy, *J. Mater. Chem.*, 2008, **18**, 615.
27 A. Lawrence, K. Trissel, M. King, Y. Zhang and A. M. Wood, *J. Oncol. Pharm. Pract.*, 2002, **8**, 27.
28 M. Chakraborty, P. Bose, T. K. Mandal, B. Dutta, T. Das, M. Mitra, J. Chakraborty and D. Basu, *Trans. Indian Ceram. Soc.*, 2010, **69**, 229.
29 S. J. Choi, J. M. Oh and J. H. Choy, *J. Ceram. Soc. Jpn.*, 2009, **117**, 543.
30 K. P. Krause and R. H. Müller, *Int. J. Pharm.*, 2001, **214**, 21.
31 M. F. Zambaux, F. Bonneaux and R. Gref, *J. Controlled Release*, 1998, **50**, 31.
32 K. Musmade, P. B. Deshpande and P. B. Musmade, *Bull. Mater. Sci.*, 2014, **37**, 951.
33 S. D'Souza, *Adv. Pharmacol.*, 2014, **1**, 5.
34 H. Wang, H. Cheng, F. Wang, D. Wei and X. Wang, *J. Microbiol. Methods*, 2010, **82**, 330.
35 R. M. Patel, V. P. Patel and S. K. Patel, *Int. J. Curr. Pharm. Res.*, 2012, **2**, 43.
36 W. P. Su, F. Y. Cheng and W. C. Su, *Int J Nanomedicine*, 2012, **7**, 4269.
37 J. M. Oh, S. H. Hwang and J. H. Choy, *Solid State Ionics*, 2002, **151**, 285.
38 M. Liqian, H. Lianbing, G. Dan, X. Xiaoyan, M. Ping and X. Yang, *Int. J. Pharm.*, 2012, **436**, 815.
39 M. Chakraborty, S. Dasgupta, C. Soundrapandian, J. Chakraborty, S. Ghosh, M. K. Mitra and D. Basu, *J. Solid State Chem.*, 2011, **184**, 2439.
40 M. Chakraborty, S. Dasgupta, P. Bose, A. Misra, T. K. Mandal, M. Mitra, J. Chakraborty and D. Basu, *J. Phys. Chem. Solids*, 2011, **72**, 779.
41 H. Murakami, Y. Kawashima, T. Niwa, T. Hino, H. Takeuchi and M. Kobayashi, *Int. J. Pharm.*, 1997, **149**, 43.
42 H. S. Panda, R. Srivastav and D. Bahadur, *Bull. Mater. Sci.*, 2011, **34**, 1599.
43 M. Chakraborty, S. Dasgupta, S. Sengupta, J. Chakraborty, S. Ghosh, J. Ghosh, M. K. Mitra, A. Mishra, T. K. Mandal and D. Basu, *Ceram. Int.*, 2012, **38**, 941.
44 I. Bala, V. Bhardwag, S. Hariharan and N. Roy, *J. Drug Targeting*, 2006, **14**, 27.
45 S. C. Lee, J. T. Oh, M. H. Jang and S. I. Chung, *J. Controlled Release*, 1999, **59**, 123.
46 J. Kang, O. Lambert, M. Ausborn and S. P. Schwendeman, *Int. J. Pharm.*, 2008, **357**, 235.
47 C. G. Pastravanua, M. Ignata and E. Popovicia, *Colloids Surf., B*, 2013, **106**, 135.
48 M. Chakraborty, P. Bose, T. K. Mandal, B. Dutta, T. Das, M. Mitra, J. Chakraborty and D. Basu, *Trans. Indian Ceram. Soc.*, 2010, **69**, 229.
49 K. Hirenkumar, I. Makadia and J. S. Siegel, *Polymers*, 2011, **3**, 1377.
50 A. R. Chamberlin, A. P. K. Cheung and P. Lim, Methotrexate, in *Analytical profile of drug substances*, ed. K. Florey, The Academic Press Inc., London, New York, Sanfrancisco, 1976, vol. 5, p. 283.
51 J. Chakraborty, S. Roychowdhury, S. Sengupta and S. Ghosh, *Mater. Sci. Eng., C*, 2013, **33**, 2168.
52 P. A. Sutton, V. Cody and G. D. Smith, *J. Am. Chem. Soc.*, 1986, **108**, 4155.
53 D. Klose, F. Siepmann, K. Elkharraz and J. Siepmann, *Int. J. Pharm.*, 2008, **354**, 95.
54 H. Kranz, N. Ubrich, P. Maincent and R. Bodmeier, *Int. J. Pharm.*, 2000, **89**, 1558.
55 J. J. Fort and A. K. Mitra, *Int. J. Pharm.*, 1990, **59**, 271.
56 L. Dian, Z. Yang, F. Li and G. Li, *Int J Nanomedicine*, 2013, **8**, 845.
57 L. Zhang, F. X. Gu, J. M. Chan, A. Z. Wang, R. S. Langer and O. C. Farokhzad, *Clin. Pharmacol. Ther.*, 2008, **83**(5), 76.
58 M. A. Tracy, K. L. Ward, L. Firouzabadian, Y. Wang, N. Dong, R. Qian and Y. Zhang, *Biomaterials*, 1996, **20**, 1057.
59 M. Vert, S. Li and H. Garreau, *J. Controlled Release*, 1991, **16**, 15.
60 B. Narashimhan, S. K. Mallapragada and N. A. Peppas, Release kinetics, data interpretation, in *Encyclopedia of Controlled Drug Delivery*, John Wiley and Sons Inc, New York, 3rd edn, 1999.
61 N. A. Peppas, *Pharm. Acta Helv.*, 1985, **60**, 110.
62 S. Dash, P. N. Murthy, L. N. Nath and P. Chowdhury, *Acta Pol. Pharm.*, 2010, **67**, 217.
63 R. Bhaskar, S. R. S. Murthy, B. D. Miglani and K. Viswanathan, *Int. J. Pharm.*, 1986, **28**, 59.
64 T. Higuchi, *J. Pharm. Sci.*, 1963, **52**, 1145.
65 J. P. Zhang, Q. Wang, X. L. Xie, X. Li and A. Q. Wang, *J. Biomed. Mater. Res., Part B*, 2010, **92**, 205.
66 X. Huang and C. S. Brazel, *J. Controlled Release*, 2001, **73**, 121.
67 B. Jakubíková and F. Kovanda, *Chem. Listy*, 2010, **104**, 906.
68 F. Danhier, E. Ansorena, J. M. Silva, R. Coco and A. L. Breton, *J. Controlled Release*, 2012, **161**, 505.

